Archives of Environmental Protection
Vol. 51 no. 4 pp. 66–77

PL ISSN 2083-4772
DOI: 10.24425/aep.2025.157229

Utilization of metallurgical dust for the adsorptive removal of the organic pollutant Reactive Red 198

Magdalena Pająk

Institute of Environmental Engineering Polish Academy of Sciences, Zabrze, Poland

Corresponding author's e-mail: magdalena.pajak@ipispan.edu.pl

Keywords: adsorption; metallurgical dust; reactive dye, wastewater, isotherms, kinetics

Abstract: The global demand for effective and sustainable water treatment technologies has intensified due to growing water scarcity and industrial pollution. Accordingly, this study evaluated the potential of unmodified metallurgical dust, a by-product of the steel industry rich in metal oxides, as a low-cost adsorbent for removing Reactive Red 198 (a representative anionic azo dye) from both synthetic aqueous solutions and real textile wastewater. This research contributes to the the development of sustainable water treatment technologies by exploring waste valorization as a strategy for pollutant removal. Batch adsorption experiments were conducted using varying concentrations of Reactive Red 198 and different doses of metallurgical dust. Both synthetic dye solutions and actual textile wastewater were tested. Adsorption performance was evaluated using nonlinear isotherm models (Langmuir, Freundlich, and Dubinin-Radushkevich) and kinetic models (Lagergren Pseudo-First-Order, Pseudo-Second-Order, and Elovich) to better understand the adsorption mechanism. The adsorption data best fitted the Freundlich and Elovich models, indicating surface heterogeneity and a chemisorption-dominated process. The maximum experimental adsorption capacity was 49.42 $mg \cdot g^{-1}$ at an adsorbent dose of 0.5 g. The material maintained high performance even under real wastewater conditions, which were characterized by elevated pH and salinity, suggesting its resilience in complex matrices. Unmodified metallurgical dust exhibits strong potential as an effective, low-cost adsorbent for anionic dye removal. Its robust performance in real wastewater underscores its practical applicability and supports the integration of environmental waste management with water pollution mitigation.

Introduction

The increasing scarcity of clean water is among the most pressing global challenges of the 21st century. Driven by rapid industrialization, population growth, urban sprawl, and the intensifying effects of climate change, freshwater resources are under mounting pressure. According to the United Nations, nearly half of the global population is expected to experience severe water stress by 2030 – unless current patterns of water use are decoupled from economic growth and significant improvements in water management and pollution control are implemented (United Nations Environment Programme, UNEP). In response, the development of efficient, low-cost, and sustainable technologies for water and wastewater treatment has become an urgent priority, not only from an environmental perspective but also in terms of public health, economic resilience, and geopolitical stability.

Parallel to this global water crisis is a growing recognition of the need to rethink industrial waste management to align with the principles of the circular economy. This paradigm shift encourages the transformation of industrial by-products, traditionally considered environmental liabilities, into value-added materials that can actively contribute to environmental remediation. Among these, metallurgical by-products such as steel slag and metallurgical dusts have gained increasing interest due to their abundance, chemical reactivity, and potential functionality in water treatment applications (Bhatnagar and Jain 2003, Jain et al. 2003, Manchisi et al. 2020, Xue et al. 2009).

In the realm of water pollution, synthetic dyes released by textile and dyeing industries represent a significant class of persistent organic pollutants. These compounds, especially azo dyes such as Reactive Red 198, are characterized by their chemical stability, vivid coloration, and resistance to conventional biological degradation pathways (Bohacz 2020, Djordjevic et al. 2014, Mustafa et al. 2025, Shaali et al. 2021). Once discharged into natural water bodies, they impair the aesthetic quality of water, reduce light penetration, hinder photosynthetic activity, and may exert toxic, carcinogenic, or mutagenic effects on aquatic organisms and humans (Asghari et al. 2023, Jain et al. 2003, Pająk 2021, Pournamdari and Niknam 2024, Xue et al. 2009).

The removal of such dyes from wastewater has been addressed through a variety of physico-chemical and biological techniques, including membrane filtration, chemical oxidation, coagulation-flocculation, and adsorption (Deogaonkar-Baride et al. 2025, Fadzli et al. 2022, Song et al. 2023). Among these, adsorption has gained prominence due to its simplicity, high removal efficiency, and flexibility in application (Bhatnagar

and Jain 2003, Pająk 2021, Shaali et al. 2021, Xue et al. 2009). However, the widespread use of activated carbon, i.e., the benchmark adsorbent, remains constrained by its high production cost and challenges related to regeneration and reuse. Consequently, there is growing interest in identifying alternative adsorbent materials that are both cost-effective and environmentally sustainable.

Reactive dyes, due to their high water solubility and resistance to conventional treatment processes, remain particularly problematic in wastewater remediation. Among them, Reactive Red 198 (RR 198) is widely used in the textile industry for dyeing cotton and cellulose-based fibers (Asghari et al. 2023, Baghapour et al. 2014, Carbaş et al. 2023, Dehghani et al. 2018, Dehghani et al. 2021, Deogaonkar-Baride et al. 2025, Kamani et al. 2024, Mustafa et al. 2025). Its molecular structure, which includes sulfonic acid groups, enhances solubility and chemical stability, making it difficult to remove through traditional biological or oxidative treatments.

Moreover, RR 198 has been detected in textile effluents in concentrations ranging from a few $mg \cdot L^{-1}$ up to several hundred $mg \cdot L^{-1}$, posing a serious environmental threat. The choice of this dye for the present study stems from both its widespread industrial application and its frequent occurrence in real textile wastewater, making it a representative model pollutant for evaluating adsorbent performance under realistic conditions.

Among the alternative materials being explored, steelmaking by-products, such as slags and metallurgical dusts, show significant promise as low-cost adsorbents for dye removal from aqueous media. Generated in large quantities during steel production, these residues are rich in metal oxides such as Fe_2O_3, CaO, MgO, Al_2O_3, and SiO_2, which are known to interact with a range of waterborne pollutants through surface adsorption and ion exchange mechanisms (Bhatnagar and Jain 2003, Makhathini et al. 2023).

In the European Union alone, approximately 16 million tons of steel slags are produced each year, with a substantial fraction still ending up in landfills or long-term storage sites, despite ongoing efforts to increase their reuse in construction and cement manufacturing (UNEP). While much of the research in this area has focused on slags, metallurgical dusts, which are often finer and with even higher concentrations of reactive metal oxides, remain underutilized (Branca et al. 2020, Chalaris et al. 2023, Makhathini et al. 2023, Simoni et al. 2024).

Due to their mineralogical composition and high density, these metallurgical dusts offer specific advantages in water treatment applications, including ease of separation from treated water and potential for pollutant binding through surface complexation and electrostatic interactions. Furthermore, their reuse in environmental applications supports circular economy principles, providing a sustainable pathway to divert industrial

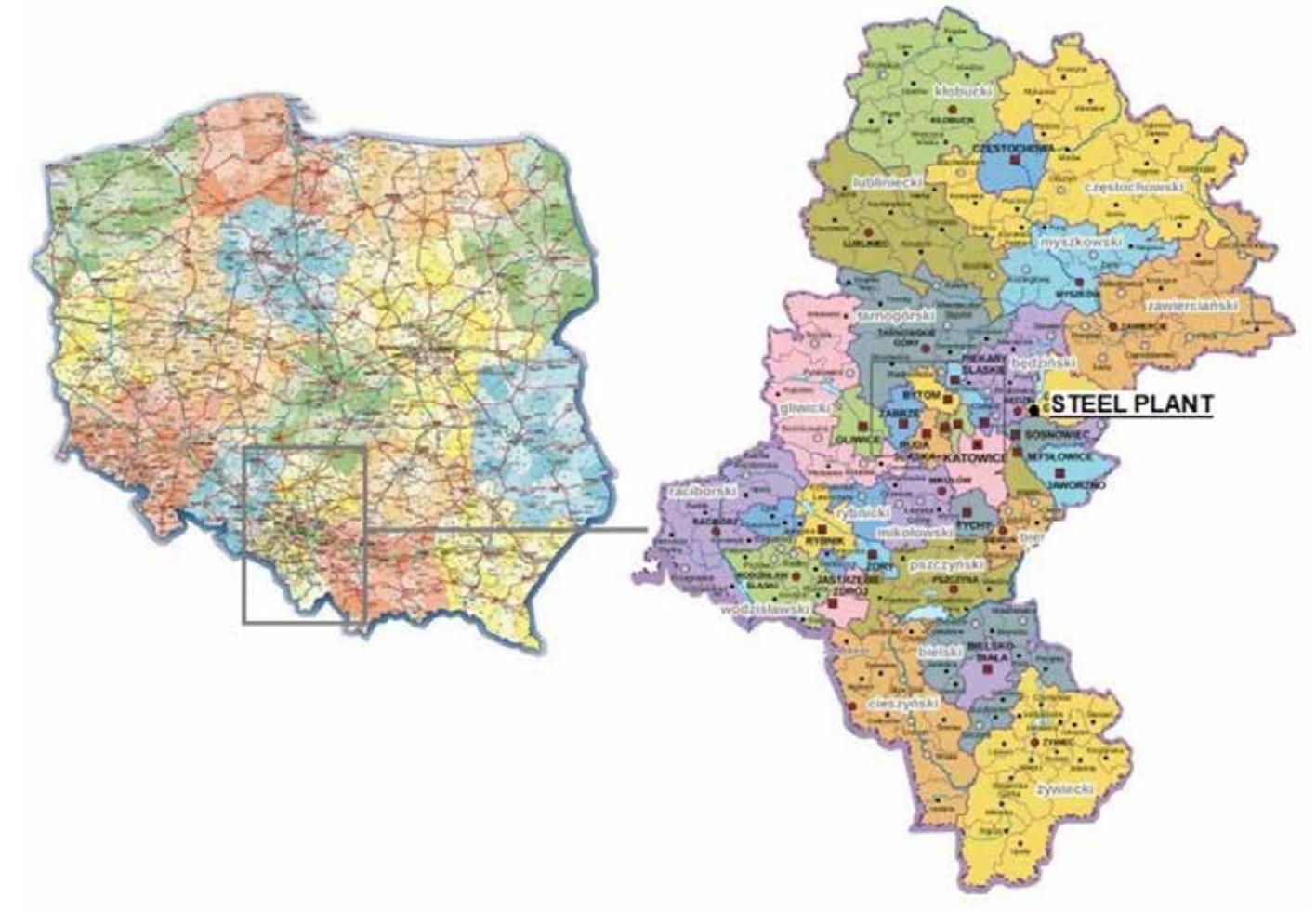

Figure 1. Location of the Steel Plant from which metallurgical dust was collected for study (www.google.com/maps)

Table 1. Composition of the textile wastewater

Textile wastewater						
COD (mg·L^{-1} O_2)	pH	Conductivity (mS·cm^{-1})	Anions (mg·L^{-1})		Cations (mg·L^{-1})	
1690	10.54	50.4	Cl	13196.70	Ca	170.40
			NO_3	58.91	K	60.70
			PO_4	<1.00	Mg	345.83
			SO_4	682.46	Na	16800.00

waste from disposal routes while addressing water pollution challenges (Matei et al. 2022).

While numerous studies focused on the removal of synthetic dyes from distilled or deionized water, real industrial wastewater presents a far more complex matrix. It often contains a mix of auxiliary chemicals, such as surfactants, salts, dispersing agents, and pH regulators, which can significantly influence the adsorption process. These substances compete with dyes for active sites or alter the surface characteristics of the adsorbent. However, to establish a reliable baseline, it was essential to begin with model solutions. This approach allowed us to isolate the effect of key process parameters such as dye concentration and adsorbent dosage. Such a stepwise approach enabled a clear understanding of fundamental interactions before applying the material to more complex, real-world scenarios. The ultimate aim was to assess the feasibility of metallurgical dust as a functional adsorbent in controlled laboratory settings, as well as to evaluate its performance in practical wastewater treatment applications.

The objective of this study was to evaluate the adsorption efficiency of metallurgical dust, a by-product of steel production, for the removal of RR 198, an anionic dye commonly used in the textile industry, from aqueous solutions and wastewater. Batch adsorption experiments were conducted to assess the impact of initial dye concentration and adsorbent dosage on removal efficiency. The equilibrium data were analyzed using several isotherm models, including Langmuir, Freundlich, and Dubinin-Radushkevich, while the adsorption kinetics were evaluated using Pseudo-First-Order, Pseudo-Second-Order, and Elovich models.

This study contributes to the growing body of knowledge on the use of low-cost, iron-rich adsorbents derived from industrial waste and demonstrates the potential of metallurgical dust for sustainable water treatment applications without requiring additional surface modifications or processing.

Materials and Methods

Preparation and characterization of the metallurgical dust

In this study, metallurgical dust samples were collected from the electrostatic precipitators of the "Kozienice" Power Plant (ENEA Kozienice Polska Power Plant), which burns hard coal (Fig. 1). The raw material was dried at 105 °C until a constant weight was achieved, then homogenized by grinding to ensure a uniform particle size distribution.

The prepared metallurgical dust samples were characterized based on their chemical composition, particle size distribution, pH, and point of zero charge (pH_{PZC}). Chemical composition was determined using X-ray fluorescence spectroscopy (XRF) with a ZSX PRIMUS II spectrometer (Rigaku, Tokyo, Japan). Particle size distribution was measured using a laser diffraction particle size analyzer (e.g., Mastersizer 2000, Malvern Instruments Ltd., Malvern, UK). The pH of the metallurgical

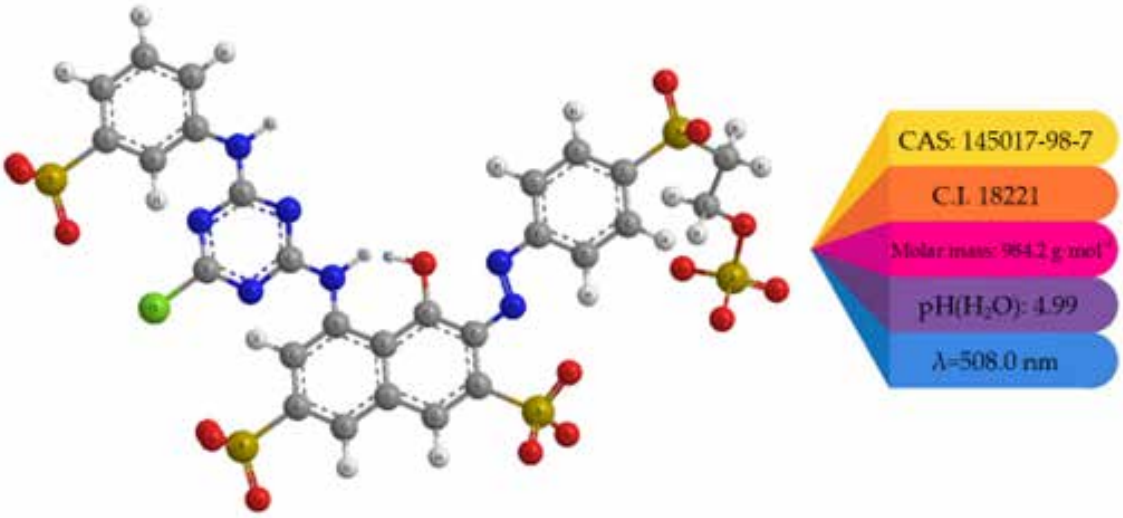

Figure 2. The characteristics of RR 198 dye

Table 2. Isotherm models and error functions used in the study

Isotherm models		
Isotherm	Nonlinear form	Reference
Langmuir	$q = \frac{q_{max} K_L C_{eq}}{1 + K_L C_{eq}}$	Langmuir 1916
Freundlich	$q = K_F \cdot {C_{eq}}^{1/n}$	Freundlich 1906
Dubinin-Radushkevich	$q = q_D \cdot exp\,(-\beta\varepsilon^2)$	Dubinin 1960
Error functions		
SSE	$\sum_{i=1}^{n} \left(q_{e,cal} - q_{e,exp}\right)_i^2$	Foo and Hameed 2010
RMSE	$\sqrt{\frac{1}{n}\sum_{i=1}^{n} \left(q_{e,exp} - q_{e,cal}\right)_i^2}$	
χ^2	$\sum_{i=1}^{n} \frac{\left(q_{e,exp} - q_{e,cal}\right)^2}{q_{e,cal}}$	

q_{max} – maximum adsorption capacity (mg·g^{-1}); K_L – Langmuir constant (L·mg^{-1}), indicates adsorbate–adsorbent affinity; K_F – Freundlich constant [(mg·g^{-1})(L·mg^{-1})^1/n], reflects capacity and intensity; 1/n – dimensionless favorability indicator; q_D – Dubinin-Radushkevich capacity (mmol·g^{-1}); β – energy-related constant (mol^2·kJ^{-2}); ε – Polanyi potential, ε = RTln(1 + 1/C_{eq}); $q_{e,cal}$ – calculated capacity; $q_{e,exp}$ – experimental capacity; n – number of data points.

dust samples was measured in deionized water at a 1:2.5 solid-to-liquid ratio using a pH meter equipped with a combination electrode (ERH-111, Hydromet, Poland).

The point of zero charge (pH_{PZC}) was determined based on the pH drift technique, following the method proposed by Calvete et al. 2009. In this method, 20.0 mL of 0.050 mol·L^{-1} NaCl solution was added to a series of Erlenmeyer flasks. The initial pH (pH_i) of each solution was adjusted between 2.0 and 10.0 using 0.1 mol·L^{-1} HCl or NaOH. The total volume in each flask was then brought to 30.0 mL by adding additional 0.050 mol·L^{-1} NaCl solution. After recording the initial pH, 50.0 mg of the adsorbent was added to each flask, which was then capped and shaken at 25 °C for 48 hours to reach equilibrium. After equilibration, the suspensions were centrifuged at 3600 rpm for 10 minutes, and the final pH (pH_f) was measured. The pH_{PZC} was determined from the point where the curve of ΔpH ($pH_f - pH_i$) versus pH_i crossed zero.

Characterization of dye

The anionic dye Reactive Red 198 (RR 198) was selected for adsorption studies. It is commonly used in the textile industry for dyeing cotton, wool, and other fibers, as well as for textile printing. Its reactivity allows it to form covalent bonds with textile fibers, rendering it highly durable and resistant to washing. The dye's chemical structure, properties, and wavelengths at which absorbance (λ) was measured are shown in Figure 2. The dye was produced by Reactive Dyes Ltd. (Bydgoszcz, Poland).

In addition to adsorption studies conducted using synthetic solutions, experiments were also performed using real textile wastewater containing RR 198, collected from dyeing facilities in the Łódź region of Poland. The characteristics of the wastewater are presented in Table 1.

Adsorption experiments

The adsorption of RR 198 dye onto metallurgical dust was examined through batch experiments conducted at ambient temperature (23 ± 2 °C). Predetermined amounts of the adsorbent (0.5 g, 1 g, or 2 g) were mixed with 100 mL of dye solution to prepare dye-adsorbent suspensions. The suspensions were agitated on a horizontal shaker at 180 rpm for 24 hours to ensure the adsorption process reached equilibrium. Upon achieving equilibrium, the adsorbent was separated from the solution by filtration.

A stock solution of RR 198 dye was prepared by dissolving the dye powder in double-distilled water and subsequently diluted to generate working solutions with concentrations ranging from 1 to 1000 mg·L^{-1} for the adsorption studies. The influence of adsorbent

concentration on dye removal efficiency was assessed using three different dosages of metallurgical dust (0.5 g, 1 g, or 2 g), to assess the. The initial (C_0) and equilibrium (C_{eq}) dye concentrations were measured using UV-Visible spectrophotometry at λ = 508 nm, the characteristic peak of RR 198. Additionally, the pH of the equilibrium solutions was recorded to evaluate the potential effects of pH variation on the adsorption process.

The amount of dye adsorbed (q) and the removal efficiency (RE) were calculated using the following equations:

$$q = \frac{(C_0 - C_{eq}) \cdot V}{m} \quad (1)$$

$$RE = \frac{(C_0 - C_{eq})}{C_0} \cdot 100 \quad (2)$$

where C_0 and C_{eq} represent the initial and equilibrium dye concentrations (mg·L^{-1}), respectively, V is the volume of the dye solution (L), and m is the mass of the adsorbent (g).

Adsorption experiments using real wastewater were conducted using five different adsorbent dosages (0.5 g, 1 g, 2 g, 5 g, and 10 g) to evaluate the removal efficiency (RE) of RR 198 under realistic conditions. All experiments were performed in triplicate to ensure the reproducibility and accuracy of the results. The resulting data were analyzed, and the mean values and standard deviations (SD) were calculated using Microsoft Office 365 software to assess data reliability and consistency.

Isotherms

To assess the maximum adsorption capacities of metallurgical dust and explore the mechanisms of RR 198 dye adsorption, three two-parameter adsorption isotherm models – Freundlich, Langmuir, and Dubinin-Radushkevich were applied. The model parameters were determined through nonlinear regression approaches, as presented in Table 2. Nonlinear regression was carried out using the classical least squares method with the Gauss-Newton algorithm in Statistica 9.0. Goodness of fit between the experimental data and the isotherm models was evaluated using three nonlinear error functions: the sum of squared errors (SSE), the root mean squared error (RMSE), and the chi-square test (χ^2), following the procedure outlined by Foo and Hameed (2010).

Table 2. Isotherm models and error functions used in the study

Kinetics

To investigate the adsorption kinetics of RR 198 dyes onto metallurgical dust, batch experiments were conducted at initial concentrations of RR 198 of 25 mg·L^{-1} and 250 mg·L^{-1}, using a single adsorbent dose of 10 g. Suspensions were agitated for varying durations – 2.5, 5, 15, 30, 60, 90, 180, 300, 720, and 1440 minutes, after which samples underwent centrifugation and filtration to isolate the supernatant. The quantity of dye adsorbed onto the metallurgical dust at each time point was calculated by subtracting the concentration of the supernatant from the initial dye concentration. Each experimental condition was performed in duplicate to ensure reliability.

To elucidate the adsorption mechanism and identify the rate-determining step, three kinetic models were applied: Lagergren pseudo-first-order (PFO), pseudo-second-order (PSO), and Elovich models. The kinetic equations used

Table 3. Kinetics equations

Kinetic model	Non-linear form	Reference
PFO	$q_t = q_e(1 - e^{-k_1 t})$	Largitte and Pasquier 2016
PSO	$q_t = \frac{k_2 q_e^2 t}{1 + k_2 q_e t}$ $h = k_2 q_e^2$	
Elovich	$q_t = 1 \cdot b^{-1} \ln(abt)$	

q_t (mg·g^{-1}) – dye adsorbed at time *t*; q_e (mg·g^{-1}) – equilibrium adsorption capacity; k_1 (1·min^{-1}) – rate constant (PFO model); k_2 (g·mg^{-1}·min^{-1}) – rate constant (PSO model); h (mg·g^{-1}·min^{-1}) – initial adsorption rate (PSO); a, b – Elovich model constants, with *a* as initial rate when $q_t \approx 0$.

are presented in Table 3. The PFO model assumes that the adsorption rate is proportional to the difference between the equilibrium adsorption capacity and the amount adsorbed at any time. The PSO model posits that the adsorption rate depends on the square of the difference between the equilibrium capacity and the amount adsorbed, suggesting that chemisorption may be the rate-limiting step. The Elovich equation, widely used to describe chemisorption processes, accounted for the exponential decrease in adsorption rate over time, influenced by both time and the amount of adsorbate present.

The suitability of each model was evaluated by comparing correlation coefficients and mean deviations, providing insights into the adsorption kinetics and the predominant mechanisms governing dye retention on metallurgical dust.

Table 4. Physicochemical properties of the metallurgical dust

Physicochemical properties	
Particle size range	0.1 – 180 μm
pH	10.11
pH_{PZC}	7.55
Fe	57.29%
FeO	7.19%
CaO	7.42%
SiO_2	6.07%
MgO	1.36%
Al_2O_3	1.21%
Mn	1.36%
Na_2O	1.48%
K_2O	0.02%
Zn	0.02%
S	0.16%

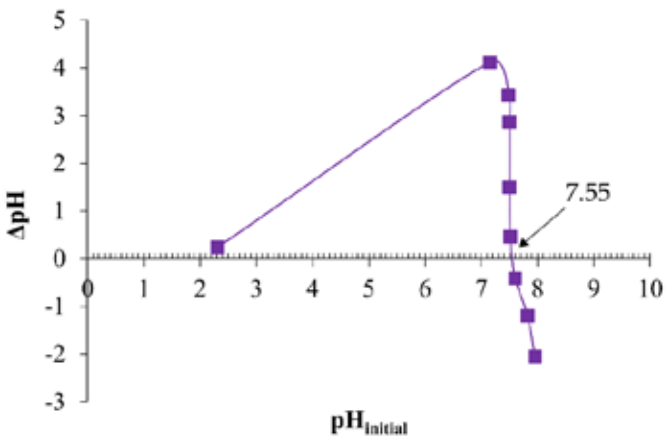

Figure 3. Point of zero charge (pH_{pzc}) of the metallurgical dust

Results

Characteristics of the metallurgical dust

The metallurgical dust used in this study originated from the sinter belt dedusting installation of a steel manufacturing plant located in the Silesian region of Poland. The metallurgical dust was collected in its raw form and then ground to achieve a fine particle size distribution ranging from 0.1 to 180 µm. The material was investigated as a potential adsorbent due to its chemical composition and buffering capacity (Pająk and Dzieniszewska 2020). Table 4 summarizes the key physical and chemical properties of the metallurgical dust.

Chemical analysis revealed a dominant presence of iron (Fe), constituting over 57% of the total mass, along with a considerable amount of iron(II) oxide (FeO). The presence of other oxides, including calcium oxide (CaO), silicon dioxide (SiO_2), magnesium oxide (MgO), and aluminum oxide (Al_2O_3), contributed to the overall reactivity of metallurgical dust and its potential for pH stabilization. The relatively high CaO content (7.42%) was especially noteworthy, as it influenced alkaline properties of the metallurgical dust.

The pH of the metallurgical dust in aqueous suspension indicated an alkaline nature. This alkalinity, supported by the presence of CaO, provided the material with significant buffering capacity, which may be beneficial in neutralizing acidic solutions (Lazarević et al. 2007). The point of zero charge, defined as the pH at which the surface of the particles carries no net electrical charge, was determined to be 7.55 using the method of Lazarević et al. (2007) and is shown in Figure 3. This parameter is important for understanding surface interactions with charged species in solution.

Adsorption of RR 198 onto metallurgical dust

The adsorption capacity (q) as a function of the equilibrium concentration (C_{eq}), along with the removal efficiency (RE) defined as the proportion of RR 198 removed relative to the initial concentration (C_0) are presented in Figure 4.

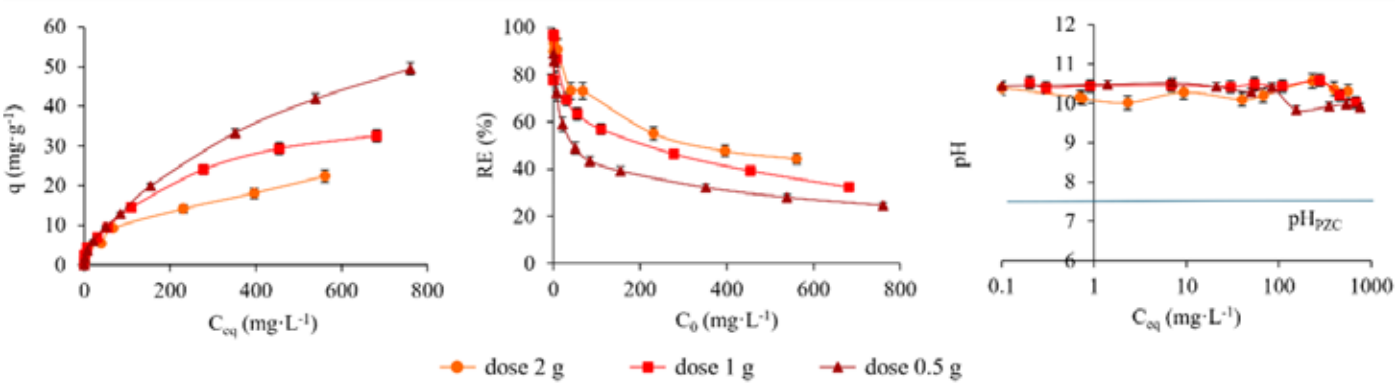

Figure 4. Adsorption capacity (q), removal efficacy (RE), and changes in the equilibrium solution pH during adsorption of RR 198 on metallurgical dust

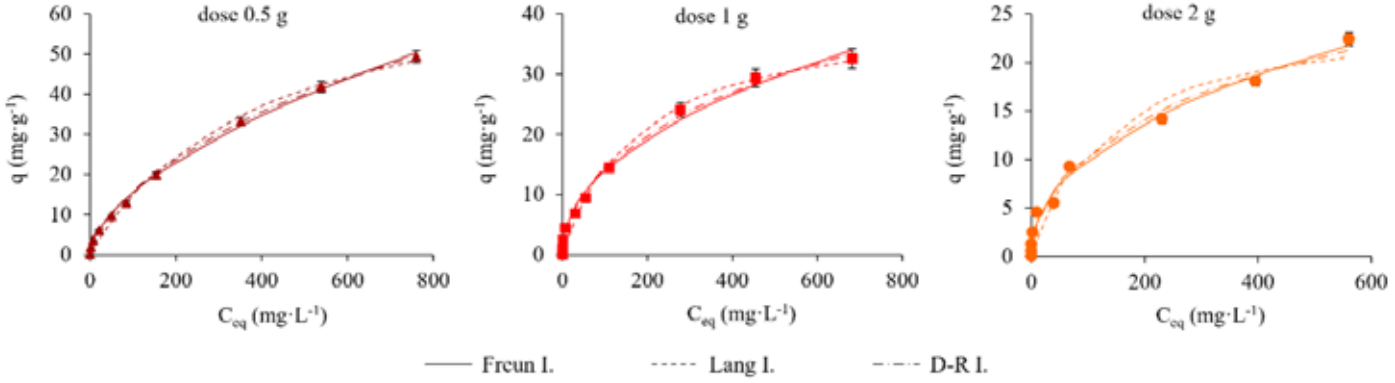

Figure 5. Comparison of experimental data with the adsorption isotherms of RR 198 onto metallurgical dust

Table 5. Isotherm parameters – nonlinear regression analysis

Adsorbent dose	0.5 g	1 g	2 g
Langmuir isotherm			
q_{exp}	49.42	32.57	22.39
Q	74.00	40.90	25.58
K_L	0.00248	0.00546	0.00730
R_L	0.2853	0.1536	0.1196
SSE	18.61	17.07	22.39
χ^2	15.62	43.33	25.74
RMSE	1.364	1.307	1.496
Freundlich isotherm			
1/n	0.5855	0.4657	0.4481
K_F	1.0362	1.6311	1.2752
SSE	4.673	10.21	5.002
χ^2	0.4431	1.705	1.567
RMSE	0.6836	1.011	0.7073
Dubinin-Radushkevich isotherm			
q_D	0.000304	0.000141	0.000085
β	0.005780	0.004438	0.004040
E	9.301	10.61	11.12
SSE	5.704	9.687	7.982
χ^2	4.302	5.848	2.592
RMSE	0.7552	0.9842	0.8934

K_F ($(mg \cdot g^{-1}) \cdot (L \cdot mg^{-1})^{1/n}$), q_{exp} ($mg \cdot g^{-1}$), Q ($mg \cdot g^{-1}$), K_L ($L \cdot mg^{-1}$)

Adsorption isotherms

The equilibrium adsorption behavior of RR 198 on metallurgical dust was evaluated using three adsorption isotherm models: Langmuir, Freundlich, and Dubinin-Radushkevich. Each model yielded key parameters that contributed to understanding the nature of the adsorption process, including surface characteristics, adsorption intensity, and energy interactions. Parameter estimation was performed using nonlinear fitting methods. Error indicators such as the sum of squared errors (SSE), root mean square error (RMSE), and chi-square (χ^2) are summarized in Table 5 to assess the goodness of fit of the applied models. Theoretical adsorption isotherms generated based on the calculated parameters are compared to experimental equilibrium data in Figure 5.

Adsorption kinetics

The kinetic behavior of RR 198 adsorption onto metallurgical dust was evaluated using three commonly employed models: the Lagergren PFO, PSO, and Elovich equations. The kinetic parameters derived from these models are summarized in Table 6, while the experimental and modeled adsorption curves are shown in Figure 6.

Adsorption of RR 198 onto metallurgical dust from textile wastewater

The results revealed that the adsorbent was capable of removing RR 198 from real textile wastewater with high efficiency. A non-linear relationship was observed between removal efficiency (RE) and adsorbent dosage, indicating that RE did not increase proportionally with increasing adsorbent mass. The highest RE occurred at a dose of 10 g (87.31%), followed by 5 g (83.73%), 2 g (74.69%). 1 g (55.04%), and 0.5 g (51.99%). The trend in removal efficiency as a function of adsorbent dosage is presented in Figure 7.

Discussion

Adsorption of RR 198 onto metallurgical dust

The adsorption of RR 198 dye onto metallurgical dust was investigated across different adsorbent dosages (0.5 g, 1 g, and 2 g), revealing strong relationship between the amount of

Table 6. The parameters of the PFO, PSO kinetic models, and Elovich equations of RR 198 adsorption on metallurgical dust

PFO model			PSO model			Elovich model		
	25 $mg \cdot L^{-1}$	250 $mg \cdot L^{-1}$		25 $mg \cdot L^{-1}$	250 $mg \cdot L^{-1}$		25 $mg \cdot L^{-1}$	250 $mg \cdot L^{-1}$
q_{exp}	2.36	12.84	q_{exp}	2.36	12.84	q_{exp}	2.36	12.84
q_1	1.745	11.97	q_2	1.892	12.48	a	9.973	8.49
k_1	0.2511	0.0387	k_2	0.0339	0.0056	b	5.635	0.6010
			h	0.1213	0.8722			
SSE	0.5483	10.73	SSE	0.8834	12.80	SSE	0.1061	5.636
RMSE	0.3329	1.158	RMSE	0.3323	1.265	RMSE	0.1152	0.8393
χ^2	0.3591	3.568	χ^2	2.2379	1.878	χ^2	0.0789	0.7042

adsorbent applied and both adsorption capacity and removal efficiency (RE). The results demonstrated that the maximum adsorption capacities were 49.42 mg·g^{-1}, 32.57 mg·g^{-1}, and 22.40 mg·g^{-1} for adsorbent dosages of 0.5 g, 1 g, and 2 g, respectively. As shown in Table 5, the highest adsorption capacity was observed at 0.5 g of adsorbent. In contrast, the removal efficiencies increased with adsorbent dosage, reaching 24.5%, 32.33%, and 44.40% for the respective dosages.

This inverse trend between adsorption capacity and adsorbent dosage is a well-documented phenomenon in adsorption studies (Xue et al. 2009). At lower dosages (e.g., 0.5 g), dye molecules were more concentrated relative to the number of available adsorption sites, leading to more efficient utilization of each gram of adsorbent. As the dosage increased, additional adsorption sites were introduced while the dye concentration remained constant. As a result, not all adsorption sites were utilized effectively, leading to a decrease in the amount of dye adsorbed per gram of metallurgical dust. However, because a greater total number of sites was available, the overall dye removal efficiency (RE) increased with adsorbent doasge. Similar trends in the influence of adsorbent dosage on RR 198 removal were also observed by Mustafa et al. (2025), who optimized various parameters for polymeric ferrite composites and confirmed the strong effect of adsorbent dosage on removal efficiency.

The adsorption experiments were conducted at solution pH values of 9.90, 10.02, and 10.03 for adsorbent dosages of 0.5 g, 1 g, and 2 g, respectively. These pH values were all above the point of zero charge (pH_{PZC}) of the metallurgical dust (7.55), indicating that the adsorbent surface carried a net negative charge under the experimental conditions. Given that RR 198 is an anionic dye, electrostatic repulsion between the negatively charged dye molecules and the negatively charged adsorbent surface would typically inhibit adsorption. Nevertheless, substantial dye removal was still observed, suggesting that additional mechanisms, such as surface complexation or coordination interactions with metal oxides (e.g., FeO, CaO, Al_2O_3), may have been involved in the binding of RR 198 to the metallurgical dust particles.

The physicochemical characteristics of the metallurgical dust further contributed to its adsorption behavior. The metallurgical dust exhibited a broad particle size distribution (0.1 – 180 µm), with finer particles likely offering greater surface area and enhancing the availability of active sites. The high Fe content (57.29%), along with the presence of FeO (7.19%), CaO (7.42%), and Al_2O_3 (1.21%), implied the presence of oxides known to interact favorably with various dye molecules via complexation or ligand exchange pathways.

The observed inverse relationship between adsorption capacity (q) and adsorbent dosage was consistent with previous studies on dye removal using industrial wastes and iron-based adsorbents (Bhatnagar and Jain 2005, Jain et al. 2003, Xue et al. 2009). Xue et al. (2009) reported a similar decrease in q with increasing dosage of modified basic oxygen furnace (BOF) slag during the removal of reactive dyes, attributing this trend to site underutilization and aggregation effects at higher solid concentrations. Bhatnagar and Jain (2005) likewise emphasized that at lower adsorbent doses, active sites tend to be more effectively utilized due to a higher dye-to-site ratio.

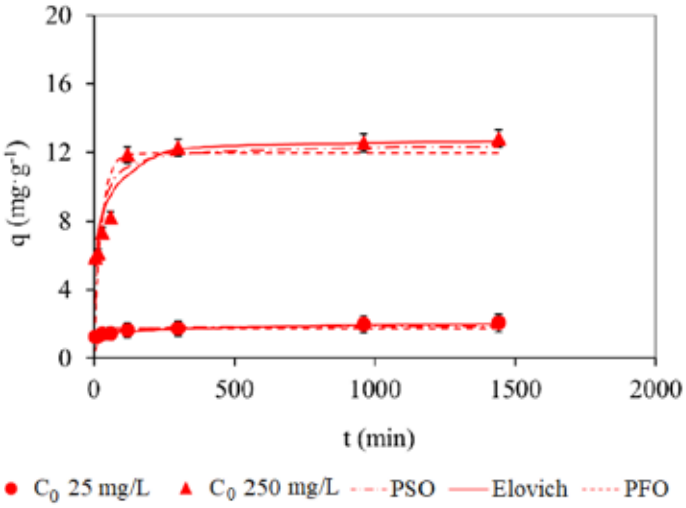

Figure 6. Comparison of experimental data with the adsorption kinetic models of RR 198 onto metallurgical dust

The relatively high removal efficiencies obtained in this study, despite the negative surface charge of the metallurgical dust above its pH_{PZC}, align with findings reported by Dehghani et al. (2021), who noted that surface complexation and interactions with metal oxides play a significant role in dye adsorption onto iron-rich substrates. The presence of metal oxides such as FeO, Al_2O_3, and CaO in the metallurgical dust used in this study supports the potential for such interactions, as highlighted by Manchisi et al. (2020) and Matei et al. (2022), who underscored the affinity of these oxides for dye molecules through mechanisms beyond simple electrostatic attraction, such as ligand exchange and complexation. Recent studies on RR198 removal using advanced adsorbents, such as Chitosan@$Fe_2(MoO_4)_3$ nanocomposites, have also confirmed that increasing the sorbent dosage enhances removal efficiency, however excessive dosages may lead to economic and environmental drawbacks, underscoring the need for dosage optimization (Pournamdari and Niknam 2024).

Adsorption isotherms

The Langmuir model, which assumes monolayer adsorption onto a homogeneous surface,−provided a satisfactory fit to the experimental data based on nonlinear regression. The

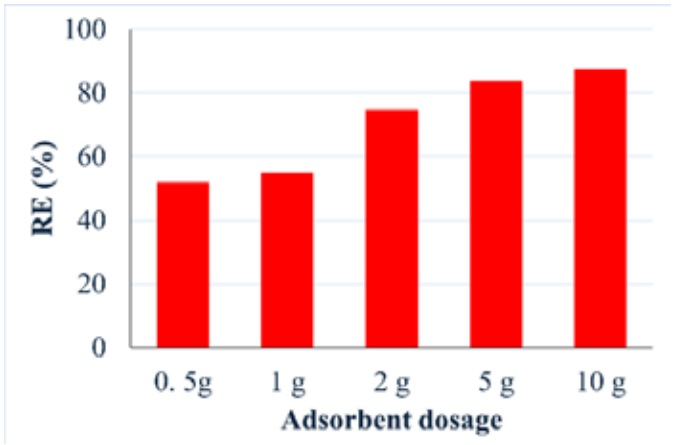

Figure 7. Removal efficacy of RR 198 from textile wastewater

maximum monolayer adsorption capacities (q) were estimated using this approach as 74.00, 40.90, and 25.58 $mg \cdot g^{-1}$ for adsorbent dosages of 0.5 g, 1 g, and 2 g, respectively, while the experimental values (q_{exp}) were 49.42, 32.57, and 22.39 $mg \cdot g^{-1}$. These discrepancies, particularly the overestimation at lower dosages, are consistent with the idealized assumptions of the Langmuir model. Nonetheless, the high R^2 values and relatively low RMSE confirm the model's applicability.

The Freundlich model, which accounts for heterogeneous surface energies, provided the best fit to the experimental data across all dosages when using nonlinear regression, as indicated by the lowest SSE, RMSE, and χ^2 values. The Freundlich constants (K_F) ranged from 1.0362 to 1.6311 $(mg \cdot g^{-1}) \cdot (L \cdot mg^{-1})^{1/n}$, indicating moderate adsorption intensity. The 1/n values (0.4481 – 0.5855) were all below 1, suggesting that the adsorption process was favorable and that the surface was energetically heterogeneous. The strong performance of the Freundlich model in describing the adsorption of RR 198 onto metallurgical dust is in agreement with findings from other studies involving reactive dyes and industrial waste-based adsorbents (Bhatnagar and Jain 2005, Jain et al. 2003, Shaali et al. 2021). Bhatnagar and Jain 2005 also reported that the Freundlich model provided the best fit for dye adsorption onto various low-cost materials, attributing this to the heterogeneous nature of the adsorbent surfaces. Similarly, Xue et al. 2009 observed a better fit of the Freundlich isotherm over the Langmuir model for BOF slag modified with polymers, especially at higher initial dye concentrations, suggesting the occurrence of multilayer adsorption.

The Dubinin-Radushkevich model, often used to distinguish between physical and chemical adsorption, also conformed well to the experimental data when fitted nonlinearly. The equilibrium concentrations and adsorption capacities were converted to SI units ($mol \cdot L^{-1}$ and $mol \cdot kg^{-1}$, respectively) prior to applying the Dubinin–Radushkevich model in order to ensure consistency in parameter estimation. The mean adsorption energy (E) values ranged from 9.301 to 11.12 $kJ \cdot mol^{-1}$, which falls within the typical range for chemisorption (8 – 16 $kJ \cdot mol^{-1}$), suggesting that chemical interactions dominated the adsorption of RR 198 onto metallurgical dust. Moreover, the higher q_D values observed at lower adsorbent dosages are consistent with the trend of greater adsorption capacities and likely reflect more efficient use of available active sites under those conditions.

Nonlinear fitting clearly captures the complexity of the adsorption process more effectively than traditional linear approaches, particularly for the Freundlich and Dubinin-Radushkevich models. The error metrics (SSE, χ^2, RMSE) further support the reliability of nonlinear methods in modeling the adsorption of RR 198 onto metallurgical dust. The chemisorption mechanism inferred from the Dubinin-Radushkevich model is further supported by Manchisi et al. 2020, who demonstrated the involvement of metal oxide surfaces in complexation reactions with dye molecules. The estimated mean adsorption energy values (E) in this study are also within the range reported by Matei et al. (2022), who examined dye adsorption on slag-derived materials and highlighted the predominance of chemical interactions, particularly under alkaline conditions. The overestimation of adsorption capacity by the Langmuir model, especially at low dosages, was also observed in studies by Dehghani et al. (2021), indicating the limitations of assuming ideal monolayer adsorption on heterogeneous materials.

In conclusion, while all three isotherm models contributed to understanding the adsorption process, the Freundlich model best described the system's behavior under nonlinear analysis. This outcome suggests a heterogeneous adsorbent surface and supports the likelihood of multilayer adsorption influenced by complex interactions beyond simple electrostatic forces. Additionally, the Dubinin-Radushkevich model indicates a chemisorption mechanism, helping to explain the effective retention of RR 198 even under conditions that might otherwise favor repulsion between dye and surface.

Adsorption kinetics

The analysis indicated that the Elovich model provided the best fit to the experimental data for both dye concentrations, as further supported by the lowest error values (SSE, RMSE, χ^2). The good performance of the Elovich model suggests that chemisorption plays a significant role in the adsorption process, likely involving heterogeneous surface interactions and a decrease in adsorption energy over time. This interpretation is consistent with findings reported by Xue et al. (2009), who demonstrated that modified basic oxygen furnace (BOF) slag followed Elovich-type kinetics during dye adsorption due to variable energy sites and complex surface interactions. Similarly, Bhatnagar and Jain (2005) emphasized the suitability of the Elovich model for dye adsorption using industrial by-products, highlighting mechanisms involving chemisorption and surface heterogeneity.

The PSO model also showed a relatively strong fit, particularly at the higher dye concentration (250 $mg \cdot L^{-1}$), where the model-estimated equilibrium adsorption capacity (q_2 = 12.48 $mg \cdot g^{-1}$) closely matched the experimental value (q_{exp} = 12.84 $mg \cdot g^{-1}$). The higher initial adsorption rate (h = 0.8722) observed at this concentration may indicate faster saturation of active sites under elevated dye loading. Nevertheless, the error values (e.g., RMSE and χ^2) for the PSO model were notably higher compared to those for the Elovich model, suggesting it was less accurate in describing the overall adsorption kinetics. The adequacy of the PSO model has also been confirmed in previous studies involving reactive dyes, such as by Dehghani et al. (2021), who applied it to systems utilizing Fe_3O_4 nanoparticles and compost ash. Their research indicated that PSO kinetics typically described systems dominanted by chemisorption, particularly under higher adsorbate concentrations – consistent with the present study.

In contrast, the PFO model showed the weakest correlation with the experimental data. Although its predicted q_1 values (1.745 and 11.97 $mg \cdot g^{-1}$) were not dramatically different from q_{exp}, the error metrics were higher, especially at the high concentration (SSE = 10.73, RMSE = 1.158). These values indicate that the PFO model was unable to accurately capture the adsorption kinetics, possibly due to its assumption of physical adsorption and limited applicability to systems involving surface heterogeneity and chemisorption. This limitation has been noted by Manchisi et al. (2020) and Matei et al. (2022), who showed that this model tends to underestimate kinetic behavior in systems with heterogeneous or chemically active surfaces, such as slags, ashes, or other metallurgical residues.

Overall, the kinetic analysis confirmed that the adsorption of RR 198 onto metallurgical dust was better described by the Elovich model, particularly due to the complex and potentially multi-mechanism nature of the process. This behavior may involve not only electrostatic and physical interactions, but also surface chemical bonding and structural rearrangement of the dye on active oxide components present in the metallurgical dust, such as FeO, CaO, and Al_2O_3.

Adsorption of RR 198 onto metallurgical dust from textile wastewater

A non-linear relationship between removal efficiency (RE) and adsorbent dosage was observed. This inverse trend was attributed to the agglomeration of particles at higher adsorbent dosages, which led to a reduction in the effective surface area and shielding of active sites available for adsorption. Similar observations have been reported in the literature by Carbaş et al. (2023) and Dehghani et al. (2018), where higher adsorbent dosages resulted in a plateau or even a decrease in dye removal efficiency due to particle overlapping and saturation effects.

Furthermore, the complexity of the matrix in real textile wastewater likely influenced the adsorption process. The sample exhibited strong alkaline conditions (pH = 10.54) and high ionic strength, as evidenced by the high conductivity (50.4 $mS \cdot cm^{-1}$) and significant concentrations of Cl^- (13196.7 $mg \cdot L^{-1}$) and Na^+ (16800 $mg \cdot L^{-1}$). These elevated salt contents caused electrostatic shielding effects, whith anions and cations competing with dye molecules for active adsorption sites on the adsorbent surface. Such effects have been documented in studies on dye removal from saline and alkaline media (Bhatnagar and Jain 2005, Pająk 2021).

Despite these challenging conditions, the adsorbent demonstrated robust performance, which indicated good selectivity and tolerance to the presence of competing ions. The high removal efficiency at low adsorbent dosages suggests that adsorption occurred via chemisorption mechanisms, potentially involving specific interactions between dye molecules and functional groups or metal oxides present in the adsorbent matrix.

Conclusions

This study evaluated the potential of metallurgical dust, sourced from a sinter belt dedusting installation at a steel plant in southern Poland, as an adsorbent for removing the anionic dye RR 198. The metallurgical dust, primarily composed of iron (over 57%) along with significant amounts of FeO, CaO, Al_2O_3, and other oxides, exhibited alkaline properties. Despite the electrostatic repulsion expected at the experimental pH values (>9.9), effective dye adsorption occurred, suggesting the involvement of mechanisms beyond simple charge attraction, such as surface complexation or coordination with metal oxides.

Adsorption performance was dosage-dependent, with lower dosages yielding higher adsorption capacities, while removal efficiency increased at higher dosages. The maximum adsorption capacity (q) reached 49.42 $mg \cdot g^{-1}$ at a 0.5 g dosage, whereas the highest removal efficiency (44.4%) was achieved at 2 g of adsorbent. Adsorption experiments were conducted at alkaline pH values (~10.0), well above the material's point of zero charge (pH_{PZC} = 7.55), confirming the likely involvement of surface-specific mechanisms. Among the isotherm models tested, the Freundlich model (fitted nonlinearly) best described the adsorption process, indicating surface heterogeneity and the likelihood of multilayer adsorption. The Dubinin-Radushkevich model further supported a chemisorption mechanism, consistent with the kinetic analysis, in which the Elovich model provided the best fit, especially under complex conditions.

Although the primary experiments were conducted using synthetic, single-component dye solutions in a batch system, preliminary tests with real textile wastewater confirmed that the material retains adsorption capacity under high-salinity and high-pH conditions. These findings suggest that the tested metallurgical dust has potential as a cost-effective adsorbent in wastewater treatment applications, especially if its performance is validated under continuous-flow and multi-contaminant conditions in future studies.

Acknowledgments

This work was supported by the Polish Ministry of Science and Higher Education (Project No. N523 3509 33) and the National Science Centre (Project No 2012/05/N/ST8/03149).

References

Asghari, A., Dalvand, S., Miresmaeili, M.S., Khoramjah, F., Omidvar, M., Kambarani, M. & Mohammadi, N. (2023). Reactive Red 198 as high-performance redox electrolyte additive for defective mesoporous carbon-based supercapacitor, *International Journal of Hydrogen Energy,* 48, 26, pp. 9776–9784. DOI: 10.1016/j.ijhydene.2022.11.322

Baghapour, M.A., Pourfadakari, S. & Mahvi, A.H. (2014). Investigation of Reactive Red Dye 198 removal using multiwall carbon nanotubes in aqueous solution, *Journal of Industrial and Engineering Chemistry*, 20, 5, pp. 2921–2926. DOI: 10.1016/j.jiec.2013.11.029

Bhatnagar, A. & Jain, A.K. (2005). A comparative adsorption study with different industrial wastes as adsorbents for the removal of cationic dyes from water, *Journal of Colloid and Interface Science*, 281, pp. 49–55. DOI: 10.1016/j.jcis.2004.08.076

Bohacz, J. (2020). Removal of a textile dye (RBBR) from the water environment by fungi isolated from lignocellulosic composts, *Archives of Environmental Protection,* 46, 2, pp. 12–20. DOI: 10.24425/aep.2020.133470

Branca, T.A., Colla, V., Algermissen, D., Granbom, H., Martini, U., Morillon, A., Pietruck, R. & Rosendahl, S. (2020). Reuse and Recycling of By-Products in the Steel Sector: Recent Achievements Paving the Way to Circular Economy and Industrial Symbiosis in Europe, *Metals*, 10, 345. DOI:10.3390/met10030345

Calvete, T., Lima, E.C., Cardoso, N.F., Dias, S.L.P. & Pavan, F.A. (2009). Application of carbon adsorbents prepared from the Brazilian pine-fruit-shell for the removal of Procion Red MX 3B from aqueous solution–Kinetic, equilibrium, and thermodynamic studies, *Chemical Engineering Journal,* 155, pp. 627–636. DOI:10.1016/j.cej.2009.08.019

Carbaş, H.Ö., Kadak, A.E., Küçükgülmez, A., Gülnaz, O. & Çelik, M. (2023). Investigation of Reactive Red 198 Dye Removal by Chitosan from Aqueous Solution, *Israeli Journal of Aquaculture - Bamidgeh*, 75, 2. DOI:10.46989/001c.88510

Chalaris, M., Gkika, D.A., Tolkou, A.K. & Kyzas, G.Z. (2023). Advancements and sustainable strategies for the treatment and management of wastewaters from metallurgical industries: an overview. *Environmental Science and Pollution Research*, 30, pp. 119627–119653. DOI:10.1007/s11356-023-30891-0

Dehghani, M.H., Pourshabanian, M. & Heidarinejad, Z. (2018). Experimental data on the adsorption of Reactive Red 198 from aqueous solution using Fe_3O_4 nanoparticles: Optimization by response surface methodology with central composite design. *Data in Brief,* 19, pp. 2126–2132. DOI:10.1016/j.dib.2018.07.008

Dehghani, M.H., Salari, M., Karri, R.R., Hamidi1, F. & Bahadori, R. (2021). Process modeling of municipal solid waste compost ash for reactive red 198 dye adsorption from wastewater using data driven approaches. *Scientific Reports*, 11, 11613. DOI:10.1038/s41598-021-90914-z

Deogaonkar-Baride, S., Koli, M. & Ghuge, S.P. (2025). Recycling textile dyeing effluent through ozonation: An environmentally sustainable approach for reducing freshwater and chemical consumption and lowering operational costs. *Journal of Cleaner Production,* 510, 10, 145641. DOI:10.1016/j.jclepro.2025.145641

Djordjevic, D., Stojiljkovic, D. & Smelcerovic, M. (2014). Adsorption kinetics of reactive dyes on ash from town heating plant, *Archives of Environmental Protection*, 40, 3, pp. 123–135. DOI: 10.2478/aep-2014-0024

Dubinin, M.M. (1960). The potential theory of adsorption of gases and vapors for adsorbents with energetically nonuniform surfaces. *Chemical Reviews*. 60, pp. 235–241. DOI:10.1021/cr60204a006

Fadzli, J., Ku Halim, K.H., Nik Him, N.R. & Puasa, S.W. (2022). A critical review on the treatment of reactive dye wastewater. *Desalination. Water Treat*. 257, pp. 185–203. DOI:10.5004/dwt.2022.28028

Foo, K.Y. & Hameed, B.H. (2010). Insights into the modeling of adsorption isotherm systems. *Chemical Engineering Journal,* 156, pp. 2–10. DOI:10.1016/j.cej.2009.09.013

Freundlich, H.M.F. (1906). Over the adsorption in solution. *Journal of Physical Chemistry*, 57, pp. 385–471

Google Maps. Available online: www.google.com/maps (accessed on 17 March 2025)

Jain, A.K., Gupta, V.K., Bhatnagar, A. & Suhas. (2003). Utilization of industrial waste products as adsorbents for the removal of dyes. *Journal of Hazardous Materials*, 101, pp. 31–42. DOI:10.1016/S0304-3894(03)00146-8

Kamani, H., Hosseinzehi, M., Ghayebzadeh, M., Azari, A., Ashrafi, S.D. & Abdipour, H. (2024). Degradation of reactive red 198 dye from aqueous solutions by combined technology advanced sonofenton with zero valent iron: Characteristics/effect of parameters/kinetic studies. *Heliyon,* e23667. DOI:10.1016/j.heliyon.2023.e23667

Langmuir, I. (1916). The constitution and fundamental properties of solids and liquids. Part I. Solids. *Journal of the American Chemical Society*, 38, pp. 2221–2295. DOI:10.1021/ja02268a002

Largitte, L. & Pasquier, R. (2016). A review of the kinetics adsorption models and their application to the adsorption of lead by an activated carbon. *Chemical Engineering Research and Design*, 109, pp. 495–504. DOI: 10.1016/j.cherd.2016.02.006

Lazarević, S., Janković-Častvan, I., Jovanović, D., Milonjić, S., Janaćković, D. & Petrović, R. (2007). Adsorption of Pb^{2+}, Cd^{2+} and Sr^{2+} ions onto natural and acid-activated sepiolites. *Applied Clay Science,* 37, pp. 47–57. DOI:10.1016/j.clay.2006.11.008

Makhathini, T.P., Bwapwa, J.K. & Mtsweni, S. (2023). Various Options for Mining and Metallurgical Waste in the Circular Economy: A Review. *Sustainability,* 15, 2518. DOI:10.3390/su15032518

Manchisi, J., Matinde, E., Rowson, N.A., Simmons, M.J.H., Simate, G.S., Ndlovu, S. & Mwewa, B. (2020). Ironmaking and Steelmaking Slags as Sustainable Adsorbents for Industrial Effluents and Wastewater Treatment: A Critical Review of Properties, Performance, Challenges and Opportunities. *Sustainability*, 12, 2118. DOI:10.3390/su12052118

Matei, E., Predescu, A.M., Șăulean, A.A., Râpă, M., Sohaciu, M.G., Coman, G., Berbecaru, A.C., Predescu, C., Vâju, D. & Vlad, G. (2022). Ferrous Industrial Wastes-Valuable Resources for Water and Wastewater Decontamination. *International Journal of Environmental Research* and *Public Health,* 19, 21, 13951. DOI:10.3390/ijerph192113951

Mustafa, G., Noreen S., Ahmad, A., Iqbal, D.N., Rizwan, M., Jilani, M.I., Ahmad, M., Munir, S. & Kennedy, J.F. (2025). Eco-friendly polymeric ferrite based on chitosan, starch, PANI, PVA, and alginate for targeted degradation of reactive Red-198 dye in wastewater treatment. *International Journal of Biological Macromolecules,* 310, 3, 142434. DOI: 10.1016/j.ijbiomac.2025.142434

Pająk, M. (2021). Adsorption Capacity of Smectite Clay and Its Thermal and Chemical Modification for Two Anionic Dyes: Comparative Study. *Water Air and Soil Pollution*, 232, 83. DOI:10.1007/s11270-021-05032-3

Pająk, M. & Dzieniszewska, A. (2020). Evaluation of the metallurgical dust sorbent efficacy in Reactive Blue 19 dye removal from aqueous solutions and textile wastewater. *Environmental Engineering Science*, 37, 7, pp. 509–518. DOI:10.1089/ees.2019.0410

Pournamdari, E. & Niknam, L. (2024). Applicability, adsorbent chitosan@Fe_2 $(MoO_4)_3$ nanocomposite for removal of textile reactive red 198 dye from wastewater. *Desalination and Water Treatment,* 317, 100268. DOI:10.1016/j.dwt.2024.100268

Shaali, A., Kamyab Moghadas, B. & Tamjidi, S. (2021). Removal of Reactive Red 198 dye from aqueous media using Boehmite/Fe_3O_4/GO magnetic nanoparticles as a novel & effective adsorbent, International *Journal of Environmental Analytical Chemistry,* 103, 18, pp. 7319–7338. DOI:10.1080/03067319.2021.1972990

Song, Y., Wang, L., Qiang, X., Gu, W., Ma, Z. & Wang, G. (2023). An overview of biological mechanisms and strategies for treating wastewater from printing and dyeing processes. *Journal of Water Process Engineering*, 104242. DOI:10.1016/j.jwpe.2023.104242

UN Environ Programme, Available online: https://www.unep.org/news-and-stories/press-release/half-world-face-severe-water-stress-2030-unless-water-use-decoupled (accessed on 19 March 2025)

Xue, Y., Hou, H. & Zhu, S. (2009). Adsorption removal of reactive dyes from aqueous solution by modified basic oxygen furnace slag: Isotherm and kinetic study. *Chemical Engineering Journal,* 147, pp. 272–279. DOI:10.1016/j.cej.2008.07.017

Wykorzystanie pyłu metalurgicznego do adsorpcyjnego usuwania zanieczyszczeń organicznych Reactive Red 198

Streszczenie. Globalne zapotrzebowanie na skuteczne i zrównoważone technologie oczyszczania wody nasila się w związku z narastającym problemem deficytu zasobów wodnych oraz postępującym zanieczyszczeniem środowiska przemysłowego. W związku z tym w niniejszym badaniu oceniono potencjał niemodyfikowanego pyłu metalurgicznego – ubocznego produktu przemysłu stalowego, bogatego w tlenki metali – jako niskokosztowego adsorbentu do usuwania barwnika reaktywnego czerwieni 198, reprezentatywnego anionowego barwnika azowego, zarówno z syntetycznych roztworów wodnych, jak i z rzeczywistych ścieków tekstylnych. Badania te wpisują się w rozwój zrównoważonych technologii oczyszczania wody poprzez wykorzystanie odpadów przemysłowych jako strategii redukcji zanieczyszczeń. Eksperymenty adsorpcyjne prowadzono w układzie okresowym, stosując różne stężenia barwnika oraz zróżnicowane dawki pyłu metalurgicznego. Testowano zarówno roztwory modelowe, jak i rzeczywiste ścieki z przemysłu tekstylnego. Skuteczność adsorpcji oceniano przy użyciu nieliniowych modeli izoterm (Langmuira, Freundlicha oraz Dubinina-Raduszkiewicza) oraz modeli kinetycznych (pseudo-pierwszorzędowego Lagergrena, pseudo-drugorzędowego i Elovicha), aby lepiej zrozumieć mechanizm procesu. Dane doświadczalne najlepiej dopasowały się do modeli Freundlicha i Elovicha, wskazując na heterogeniczność powierzchni oraz dominującą rolę chemisorpcji. Maksymalna pojemność adsorpcyjna wyniosła 49,42 $mg \cdot g^{-1}$ przy dawce adsorbentu 0,5 g. Materiał zachował wysoką skuteczność również w warunkach rzeczywistych ścieków, charakteryzujących się podwyższonym pH i wysokim zasoleniem, co potwierdza jego odporność w złożonych matrycach. Niemodyfikowany pył metalurgiczny wykazuje duży potencjał jako skuteczny i tani adsorbent do usuwania barwników anionowych. Jego stabilna efektywność w rzeczywistych ściekach podkreśla praktyczną przydatność materiału i wspiera koncepcję łączenia gospodarki odpadami przemysłowymi z działaniami na rzecz ograniczania zanieczyszczenia wód.